BBA - Molecular Basis of Disease 1871 (2025) 167523

Contents lists available at ScienceDirect

BBA - Molecular Basis of Disease

journal homepage: www.elsevier.com/locate/bbadis

Phosphorylation of BRCA1 at serine 1387 plays a critical role in cathepsin S-mediated radiation resistance via BRCA1 degradation and BCL2 stabilization

Gil-Im Mun [a,1], Eun Choi [a,1], Hee Jin [a,1], Seul-Ki Choi [a], Hanhee Lee [a], Seoyoung Kim [a,b], Junghyun Kim [d], Chaerin Kang [a], Hye Lim Oh [a], Hae-June Lee [c], Dae-Ro Ahn [d], Yun-Sil Lee [a,*]

[a] Graduate School of Pharmaceutical Sciences, Ewha Womans University, Seoul 03760, Republic of Korea
[b] New Horizon Cancer Institute, Myongji Hospital, Seoul 10472, Republic of Korea
[c] Division of Basic Radiation Bioscience, Korea Institute of Radiological and Medical Sciences, Seoul 01812, Republic of Korea
[d] Chemical and Biological Integrative Research Center, Korea Institute of Science and Technology (KIST), Hwarangno 14-gil 5, Seongbuk-gu, Seoul 02792, Republic of Korea

A B S T R A C T

There is evidence that BRCA1, particularly cytoplasmic BRCA1, plays a significant role in initiating apoptosis through various mechanisms. Maintaining the stability of BRCA1 in cancer cells may be a promising therapeutic strategy for breast cancer, especially in cases of triple-negative breast cancer (TNBC) lacking appropriate therapeutic targets. Previously, it was reported that cathepsin S (CTSS) interacts with the BRCT domain of BRCA1, leading to ubiquitin-mediated degradation. We further investigated the critical role of BRCA1 phosphorylation at Ser1387, which is mediated by ionizing radiation (IR)-induced activation of ATM. This phosphorylation event was identified as a key factor in CTSS-mediated ubiquitin degradation of BRCA1. The functional inhibition of CTSS, using small molecules or a knockdown system, sensitized TNBC cells when exposed to IR by restoring the stability of cytoplasmic BRCA1. The increase in cytoplasmic BRCA1 led to the degradation of anti-apoptotic BCL2, which was responsible for the radiosensitization effect observed with CTSS inhibition. These results suggest that inhibiting CTSS may be an effective strategy for radiosensitization in TNBC cells through BCL2 degradation that is mediated by inhibition of CTSS-induced BRCA1 degradation.

1. Introduction

Triple negative breast cancer (TNBC) refers to a subset of tumors (10–20 %) that lack the expression of estrogen receptor (ER), progesterone receptor (PgR), and HER2. Due to the absence of these markers, extensive efforts have been made to identify actionable molecular targets for treating triple negative breast tumors. Germline mutations in BRCA1 are found in approximately 10 % of TNBC patients [1,2]. In addition to germline mutations, alternative mechanisms such as promoter methylation, somatic BRCA1 mutations, and gene deletion have been identified to impair the function of BRCA1. These mechanisms contribute to the presence of "BRCAness" genotypes, which describes tumors that exhibit a biological and clinical phenotype similar to tumors with BRCA1 mutations, even in their absence. Functional deficiency, similar to germline BRCA1 mutations, can be observed in BRCA1-proficient TNBC, such as that with low expression of BRCA1, which is another form of BRCAness [3,4]. Hence, it is crucial to identify novel targets to overcome BRCAness, particularly in cases of TNBC with functional deficiency.

Various serine residues (S988, S1189, S1387, S1423, S1457, S1524, and S1542) within BRCA1 can be phosphorylated by Chk1, Chk2, ATR, or ATM [5–10]. While some studies have provided insights into the physiological significance of these events, the specific mechanistic implications and functional consequences of individual phosphorylations in BRCA1 remain largely unexplored. The stability of the BRCA1 protein is regulated by an ubiquitin-proteasome mechanism [11]. A recent study showed that BRCA1 phosphorylation is involved in its molecular stability [12]. Therefore, biochemical investigations focused on dissecting the molecular events following BRCA1 phosphorylation could lead to the development of compounds that restore BRCA1 deficiency.

Among the various functions of BRCA1 and its role in genomic stability, we drew our attention to its involvement in apoptosis. Numerous studies have provided evidence for the significant role of BRCA1, particularly cytoplasmic BRCA1, in the initiation of apoptosis through

* Corresponding author at: College of Pharmacy, Ewha Womans University College of Pharmacy, 52, Ewhayeodae-gil, Seodaemun-gu, 03760 Seoul, Republic of Korea
E-mail address: yslee0425@ewha.ac.kr (Y.-S. Lee).
[1] These authors are co-first authors.

https://doi.org/10.1016/j.bbadis.2024.167523
Received 17 January 2024; Received in revised form 19 August 2024; Accepted 17 September 2024
Available online 25 September 2024
0925-4439/© 2024 The Authors. Published by Elsevier B.V. This is an open access article under the CC BY-NC-ND license (http://creativecommons.org/licenses/by-nc-nd/4.0/).

diverse mechanisms [13]. One of these mechanisms involves the interplay between BRCA1 and anti-apoptotic BCL2 proteins. Nuclear BRCA1 facilitates the production of BCL2, whereas cytosolic BRCA1 enhances the degradation of BCL2 via proteasomes [14]. This information elucidates the crucial role of cytosolic BRCA1 in triggering apoptosis when DNA damage occurs.

In our previous study, we found that cathepsin S (CTSS), a lysosomal enzyme induced by DNA damage, degrades the BRCA1 protein, which is associated with radiation (IR) resistance in breast cancer cells [15]. Elevated CTSS expression has been linked to TNBC, high-grade, and late-stage breast cancer [16]. CTSS recognizes the BRCT domain within BRCA1, resulting in ubiquitination-mediated degradation of BRCA1. This degradation ultimately contributed to the promotion of tumorigenesis and inhibition of cell death [15]. Thus, inhibiting CTSS to improve BRCA1 stability may serve as a promising therapeutic strategy for breast cancer treatment. In this study, we further investigated the precise mechanism through which CTSS promotes the degradation of cytoplasmic BRCA1 in TNBC, with a specific emphasis on apoptosis.

2. Results

2.1. CTSS inhibition led to radiosensitization in TNBC cells through BRCT domain-mediated BRCA1 stabilization

In this study, we examined the protein expressions of both BRCA1 and CTSS across diverse TNBC cell lines. The TNBC cell lines that carry the wild-type (WT) BRCT domain of *BRCA1*, designated as WT cells, include MDA-MB-231 (231), MDA-MB-453 (453), and HCC70 [4]. The TNBC cell lines that have a mutated (MT) BRCT domain of *BRCA1*, termed MT cells, include MDA-MB-436 (436) and HCC1937 (1937). Among the WT cells, 231 cells displayed heightened BRCA1 level and decreased CTSS expression compared to 453 and 70 cells. The 453 cells exhibited a higher level of the CTSS precursor form than its mature counterpart, while 70 cells showed an elevated level of mature CTSS. This distinction indicates a converse relationship between CTSS and BRCA1 protein levels within the WT cells. Conversely, in the MT cells, BRCA1 protein level was undetectable when using a C-terminal antibody; 436 cells showed higher CTSS expression than 1937 cells (Supplementary Fig. S1A). The subsequent experiment aimed to determine cell sensitivity to IR. Among the WT cells, 231 cells showed a higher level of cell death in response to IR than did 453 and 70 cells. However, with MT cells, there was no significant difference in cell death despite variations in CTSS expression (Supplementary Fig. S1B). To investigate the involvement of BRCA1 expression in IR sensitivity with or without CTSS, inhibition of CTSS using either siRNA targeting *CTSS* (si*CTSS*) or the CTSS inhibitors, RO5461111 (RO) and *Z*-FL-COCHO (ZFL). Inhibiting CTSS resulted in elevated expression of BRCA1. Upon exposure of TNBC cells to IR, regardless of the mutation status of the BRCT domain, increased cleavage of PARP1 was observed. Moreover, when CTSS was inhibited in the WT cells, the BRCA1 protein level was potentiated, as

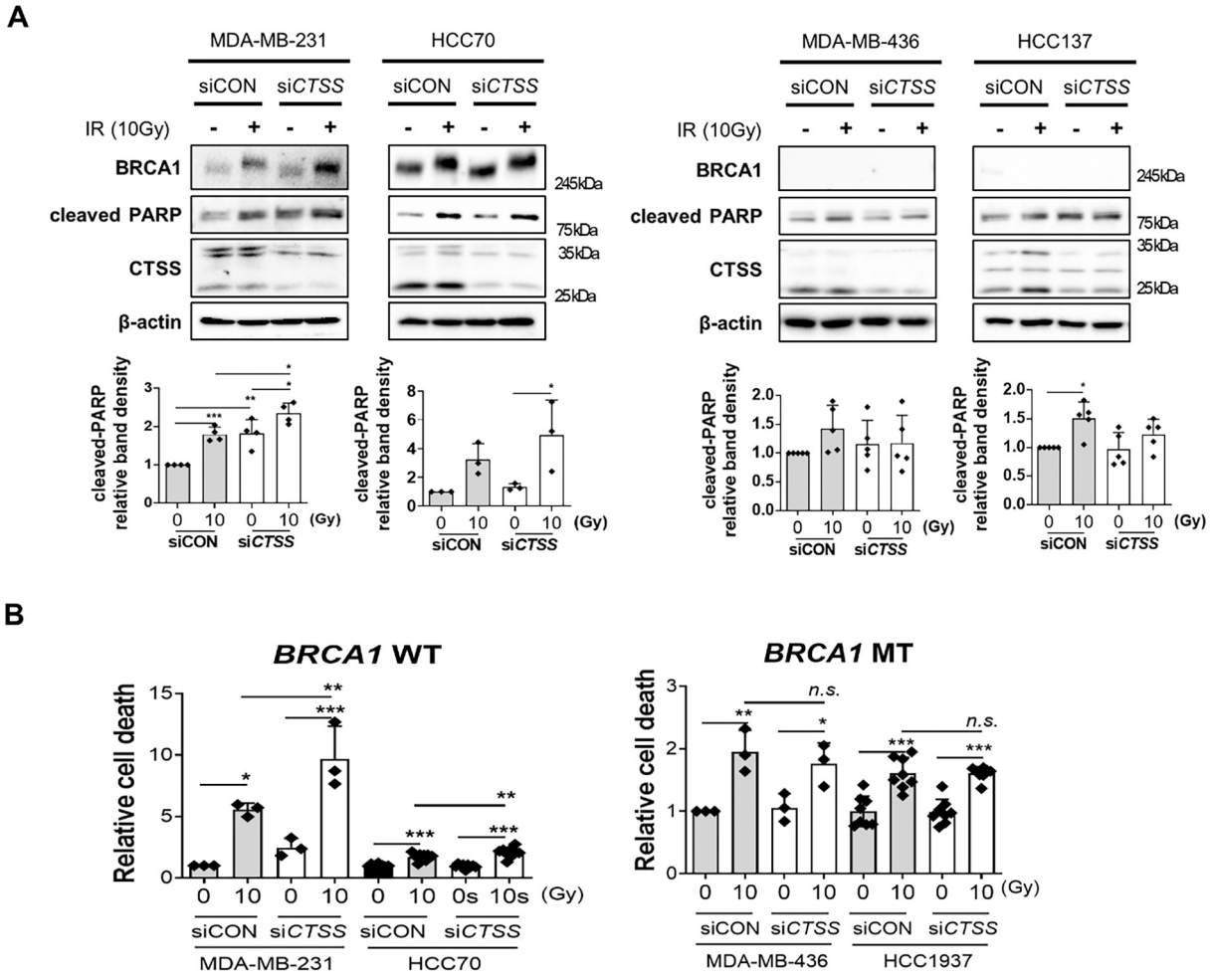


Fig. 1. Knock-down of *CTSS* enhanced BRCA1 level and increased the sensitivity to radiation in TNBC cells harboring wild-type BRCA1.
TNBC cell lines transfected with *CTSS* specific siRNAs (si*CTSS*) were exposed to irradiation (10 Gy). TNBC cell lines with wild-type BRCA1 (WT); MDA-MB-231 (231) & HCC70 and with mutant BRCA1 (MT); MDA-MB-436 (436) & HCC1937 (1937). (A) Western blot analysis and the quantification of cleaved-PARP1 induction; (B) Cell death was evaluated with PI staining. Results are the means and SD (*$p < 0.05$, ANOVA).

was IR-induced PARP1 cleavage and cell death. The sensitization effects achieved through the combination of IR with si*CTSS* or CTSS inhibitors were more pronounced in 231 cells than in 70 cells. However, in MT cells, inhibition of CTSS did not increase the IR-mediated PARP1 cleavage (Fig. 1A and Fig. 2A) or cell death (Fig. 1B and Fig. 2B).

CTSS controlled the stability of BCL2 through its interaction with BRCA1 in the cytoplasmic fraction.

While BRCA1 was primarily localized to the nucleus, a portion was also detected in the cytoplasm. Conversely, CTSS was predominantly situated in the cytoplasm. Suppression of CTSS using si*CTSS* resulted in a more pronounced restoration of cytoplasmic BRCA1 compared to nuclear BRCA1 (Fig. 3A). To explore the interplay between BRCA1 and CTSS, a proximity ligation assay (PLA) was conducted to detect protein-protein interactions with single-molecule precision in situ. The PLA targeting CTSS-BRCA1 exhibited numerous red puncta in both the nucleus and cytoplasm, with a notable abundance in the cytoplasm of 231 cells. Importantly, si*CTSS* treatment reduced these red puncta in both cellular compartments (Fig. 3B). Functioning as an E3 ligase, BRCA1 is recognized for its role in modulating the stability of BCL2, which is a key inhibitor of apoptosis [14]. Consequently, si*CTSS* or sh*CTSS* intervention led to a decrease in BCL2 expression and concomitant restoration of BRCA1 expression (Fig. 3C). Furthermore, when treated with cycloheximide (CHX), si*CTSS* expedited the degradation of BCL2 protein, which shortened the protein half-life (Fig. 3D). Immunoprecipitation analysis revealed a more pronounced interaction between BRCA1 and BCL2 in cells transiently transfected with si*CTSS*. This interaction shift was accompanied by a reduction in BCL2 expression and a concurrent increase in BRCA1 expression (Fig. 3E). Furthermore, overexpressing WT-BRCA1 led to a decrease in BCL2 level, while treating sh*CTSS* cells with si*BRCA1* reinstated BCL2 expression (Fig. 3F). To deepen our understanding of the BRCA1-BCL2 interaction, a PLA assay was employed. The outcomes indicated that cells with stable sh*CTSS* transfection exhibited a more robust BRCA1-BCL2 interaction than did shCON cells (Fig. 3G). Exposure of WT cells to IR resulted in an increased BCL2 level, but the level decreased upon exposure to si*CTSS* or CTSS inhibitors (RO and ZFL) (Fig. 3H and I). In an in vivo xenograft model employing WT cells (231 cells), tumors transfected with sh*CTSS* exhibited diminished BCL2 expression and elevated BRCA1 expression compared to shCON tumors, when they were detected by immunohistochemistry (IHC). Additionally, sh*CTSS* tumors displayed fewer Ki67-positive cells, which is indicative of reduced proliferation (Fig. 3J and K).

2.2. *CTSS recognized phosphorylated BRCA1 at S1387, prompted its degradation and suppressed BRCA1-mediated tumor apoptosis*

BRCA1 phosphorylation at specific sites, namely Ser1387, Ser1423, and Ser1524, has been documented following exposure to IR and is known to impact BRCA1 stability. It is reasonable to conjecture that

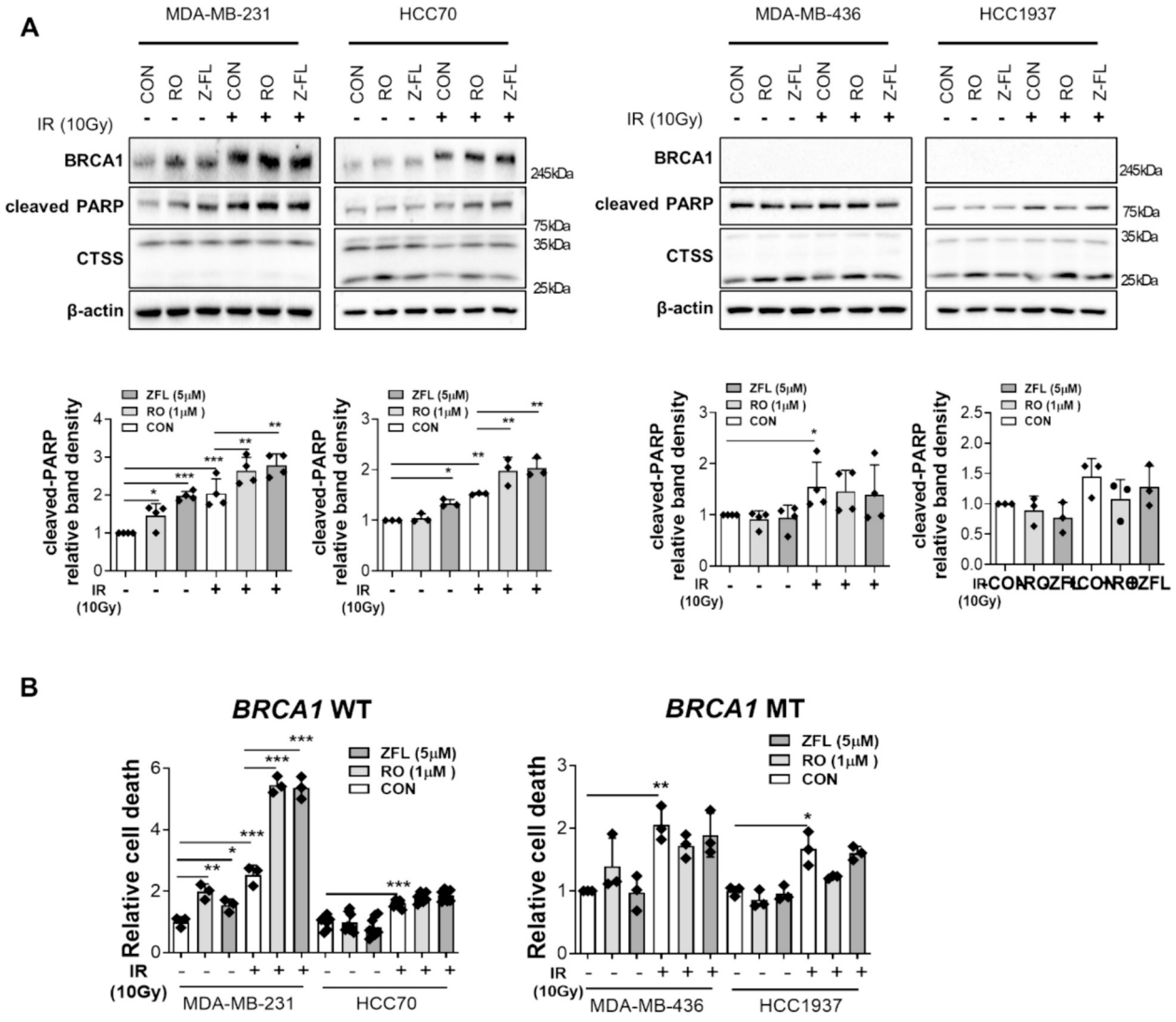


Fig. 2. CTSS inhibitors enhanced BRCA1 level and increased the sensitivity to radiation in TNBC cells harboring wild-type BRCA1.

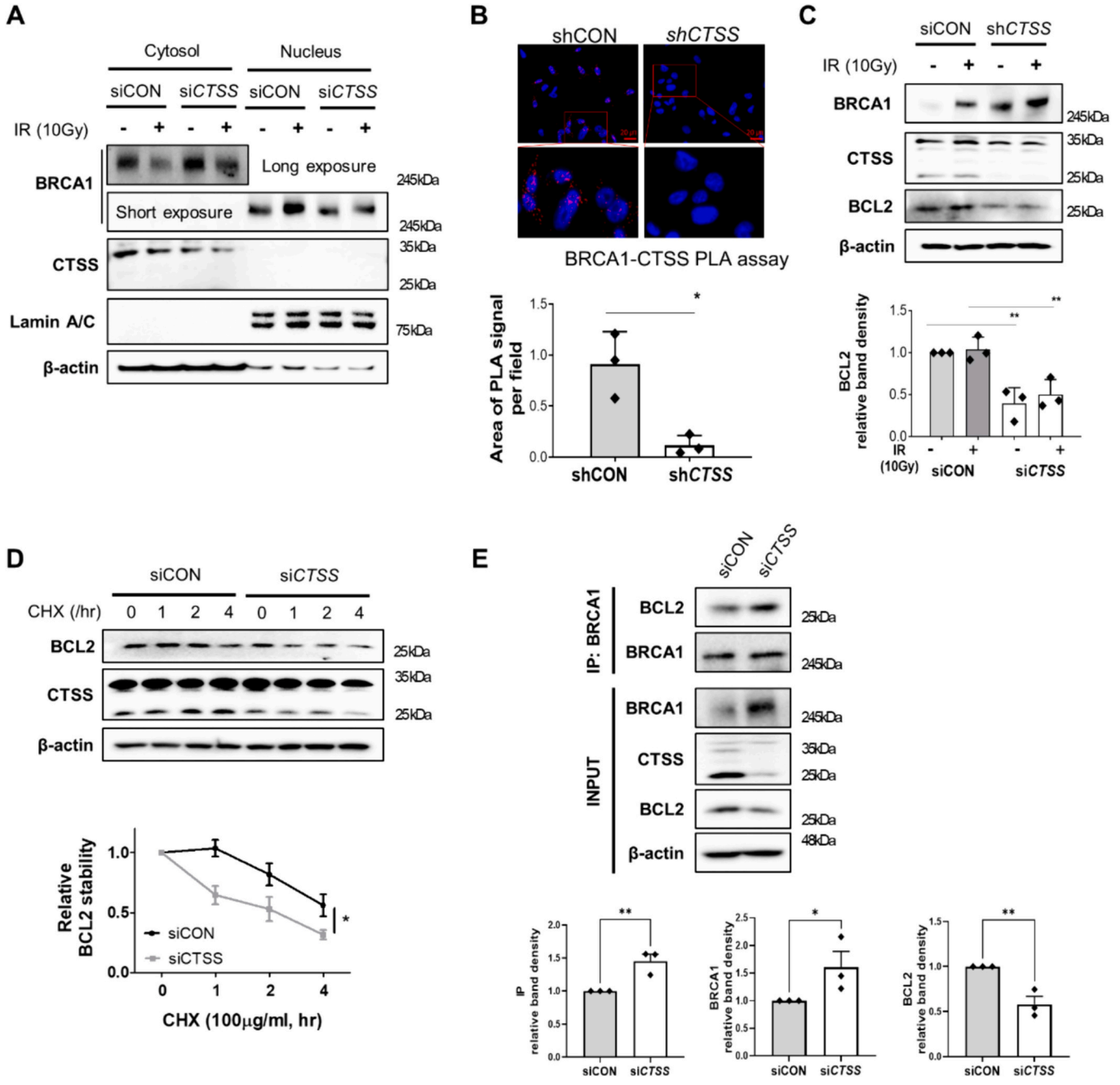


Fig. 3. Knock-down of CTSS restored cytosolic BRCA1 and down-regulated the protein stability of BCL2 through the interaction with BRCA1.
(A-J) MDA-MB-231 cells either transiently transfected with si*CTSS* or stably transfected with sh*CTSS* were used. (A) Western blot analysis of cytosolic and nuclear fractions from MDA-MB-231 cells after the exposure to irradiation (10 Gy). Fraction purity and equal loading were assessed by Lamin A/C and β-actin.; (B) BRCA1-CTSS proximity ligation assay (PLA) analysis and the quantification of PLA signals; (C) Western blot analysis and the quantification of BCL2; (D) Cycloheximide (CHX) chase assay was performed to detect BCL2 protein level after the treatment with 100 μg/mL for various lengths of time.; (E) Co-immunoprecipitation (IP) assay was performed to detect the interaction between BRCA1 and BCL2 influenced by the presence of CTSS.; (F) Western blot analysis of MDA-MB-231 stable cell lines after the transfection with wild-type BRCA1 (BRCA1 WT) DNA constructs or *BRCA1* specific siRNAs (si*BRCA1*).; (G) BRCA1-BCL2 PLA analysis and the quantification of PLA signals; (H-I) MDA-MB-231 cell line and HCC70 cell line were used. Western blot analysis of BRCA1 and BCL2 in cells exposed to irradiation (10 Gy) after (H) the transient transfection with si*CTSS* or (I) the pre-treatment with CTSS inhibitors. (J) Representative images of immunohistochemistry (IHC) analysis and (K) quantifications of CTSS, BRCA1, BCL2 and Ki67 positive areas in tumor xenograft model. Results are the means and SD or SEM (*$p < 0.05$, Student's *t*-test or ANOVA).

CTSS could potentially recognize distinct phosphorylation sites on BRCA1. Indeed, 10 Gy IR led to heightened phosphorylation of BRCA1 at S1524, S1423, and S1387 (Supplementary Fig. S2A). Moreover, ATM deficient cells to hinder BRCA1 phosphorylation resulted in the restoration of BRCA1 expression. This finding suggests that CTSS-facilitated BRCA1 degradation hinges on phosphorylation (Fig. 4A). Blocking protein phosphatase 2A (PP2A) with LB100 induced increased phosphorylation of BRCA1 and accelerated BRCA1 degradation, but these effects decreased when sh*CTSS* was employed, indicating the involvement of BRCA1 phosphorylation in CTSS-mediated BRCA1 degradation

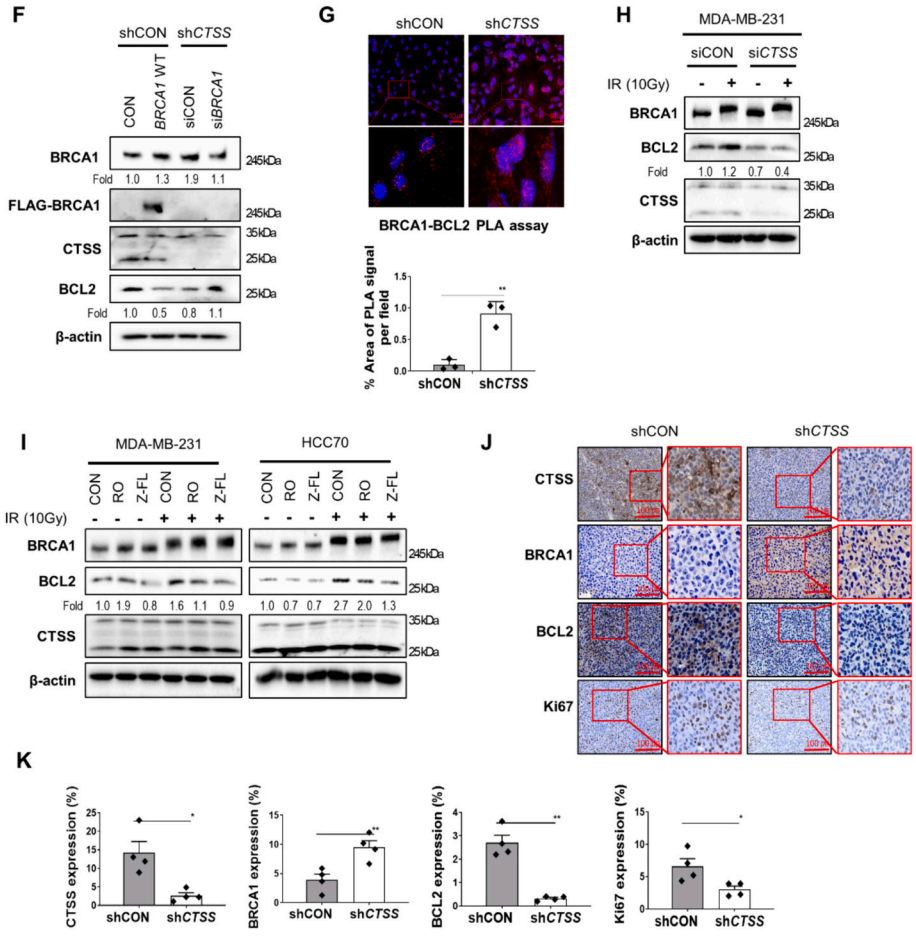


Fig. 3. (*continued*).

(Fig. 4B). Conversely, in the context of increased dephosphorylation of BRCA1 by pyrophosphatase (PPase) treatment, CTSS induced-BRCA1 degradation was partially hindered (Supplementary Figs. S2B).

To explore whether specific phosphorylation sites on BRCA1 play a role in its degradation by CTSS, mutants were engineered with either phospho-defective or phospho-mimicking alterations at each serine phosphorylation site. The phospho-defective mutants, including S988R, S1523R, and S1423R (where serine was replaced with arginine), induced BRCA1 degradation similar to WT-BRCA1 overexpression. However, S1387R, the phospho-defective mutant at S1387, did not exhibit BRCA1 degradation by CTSS (Supplementary Fig. S2C). In parallel, the phospho-defective mutant S1387A (where serine was replaced with alanine) did not incite BRCA1 degradation through CTSS, in contrast to both BRCA1 WT and S1423A (Figs. 4C). Moreover, the immunoprecipitation analysis revealed that the phospho-defective mutant S1387A exhibited diminished interaction between BRCA1 and CTSS and a consequent decrease in BRCA1 degradation (Supplementary Fig. S2D). Cells subjected to CTSS knockdown of the CRISPR-Cas9 system displayed elevated level of phosphorylated BRCA1 at S1387, along with an overall increase in total BRCA1 expression (Supplementary Fig. S2E). Furthermore, in comparison to S1387E, BRCA1 S1387A demonstrated an extended half-life (Fig. 4D). Notably, BRCA1 S1387A led to decreased BCL2 expression, while S1387E provoked an increase (Fig. 4E). With regard to *gadd45* promoter activity, cells with CTSS knockdown exhibited greater activity in comparison to shCON. Both WT-BRCA1 and S1387E displayed higher *gadd45* activity than shCON cells. Notably, this effect was more pronounced in sh*CTSS* cells. However, the S1387A mutant of BRCA1 exhibited no disparity in *gadd45* promoter activity between shCON and sh*CTSS* cells (Fig. 4F). Additionally, unlike S1387E, S1387A contributed to heightened radiosensitivity, as evidenced by PARP1 cleavage, γH2AX expression, and cell death (Fig. 4G and H).

2.3. *CTSS inhibition led to increased sensitivity to IR in a xenograft mouse model using TNBC cells harboring WT BRCA1*

In this study, 231 cells were xenografted, and a CTSS inhibitor (RO) was administered alongside IR, both in the presence and absence of functional CTSS (Fig. 5A). The tumor growth delay induced by IR was notably more pronounced in the shCON tumors than it was in the sh*CTSS* tumors (Fig. 5B). Furthermore, intraperitoneal administration of RO resulted in enhanced radiosensitivity in the shCON tumors. Conversely, this radiosensitization effect was absent in the sh*CTSS* tumors (Fig. 5C). IHC analysis targeting Ki67, a proliferation marker, revealed that the combined treatment of IR and RO led to a reduction in Ki67 staining specifically in the shCON tumors. In contrast, no such reduction was observed in the sh*CTSS* tumors (Fig. 5D). We also conducted immunostaining to examine the expression of CTSS, BRCA1, and BCL2 in each group. The sh*CTSS* tumors demonstrated an increase in BRCA1 stability in comparison to the shCON tumors. When combined with IR, CTSS inhibition by RO caused a more pronounced increase in BRCA1 expression in the shCON tumors. However, in the sh*CTSS* tumors, no additional enhancement of BRCA1 expression was noted with RO treatment in combination with IR. Furthermore, the increase in BCL2 expression by IR was repressed by RO treatment in the tumor tissues of shCON xenograft mice. This inhibitory effect was absent in the tumor tissues of sh*CTSS* xenograft mice. This finding underscores the importance of activation pathways triggered by IR, such as those involving

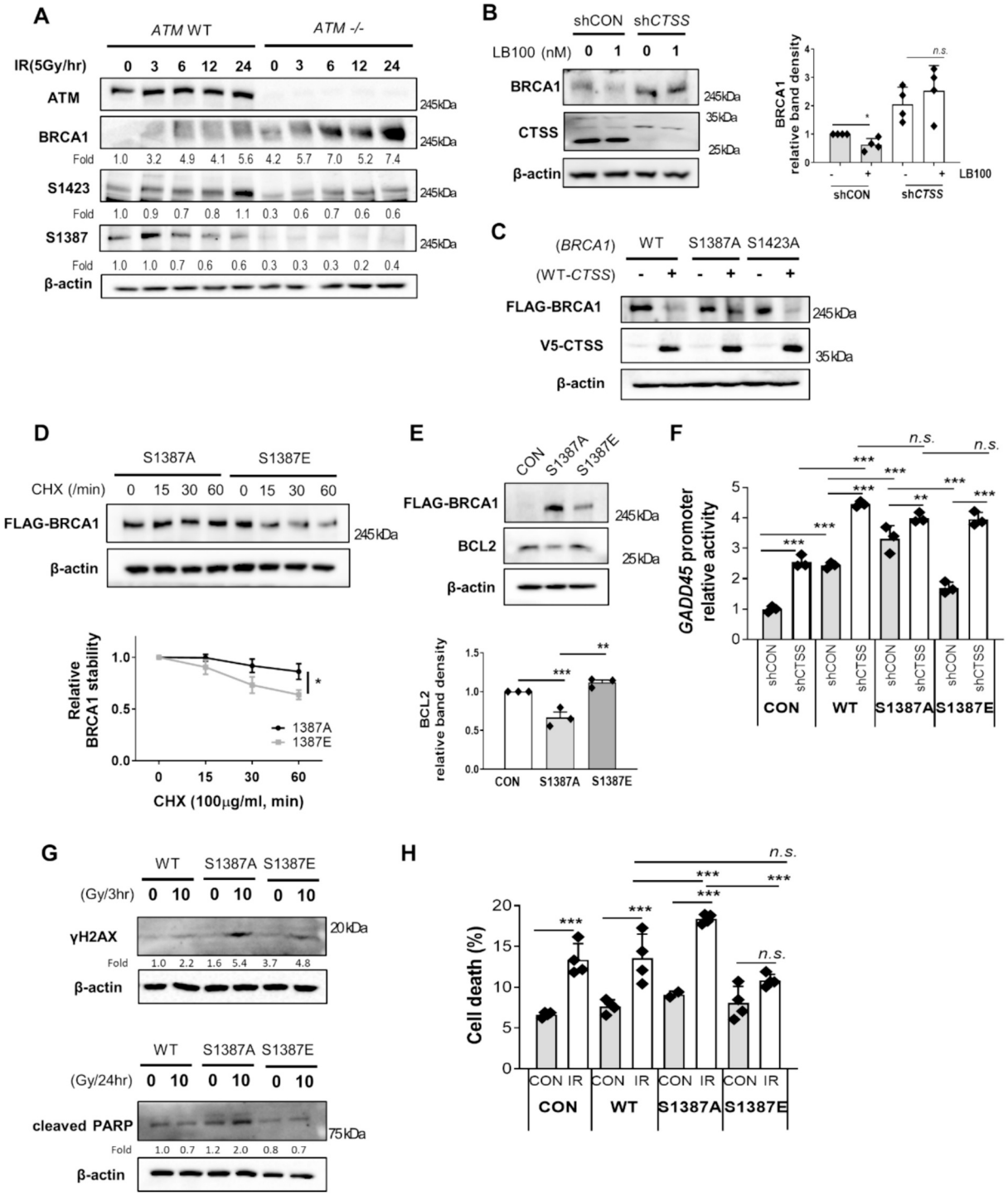


Fig. 4. CTSS specifically recognized phosphorylated BRCA1 at S1387 and repressed BRCA1-mediated cell death after irradiation.
(A) Western blot analysis of time-dependent change in ATM-proficient GM00637 and ATM-deficient GM05849 fibroblast cells after irradiation (10 Gy).; (B) Western blot analysis and quantification of BRCA1 levels in MDA-MB-231 cells stably transfected with sh*CTSS* after treatment with LB100. LB100, a protein phosphatase 2A (PP2A) inhibitor, accerlerated phosphorylation of BRCA1.; (C-G) MDA-MB-231 cells were transfected with flag-tagged point mutants of BRCA1 at S1387 (phospho-defective; A and phopspho-mimicking replacement of serine with glutamate; E); (C) Cycloheximide (CHX) chase assay was performed to detect BRCA1 protein level after the treatment with 100μg/mL for various lengths of time. (D) Western blot analysis and the quantification of BCL2; (E) GADD45 promoter activity was measured in MDA-MB-231 stable cell lines. (F) Western blot analysis of DNA damage and cell death markers (γH2AX and cleaved parp) at the indicated times after irradiation (10 Gy); (G) Cell death was evaluated with PI staining. Results are the means and SD or SEM (*$p < 0.05$, Student's *t*-test or ANOVA).

ATM-mediated BRCA1 phosphorylation, for CTSS-mediated BRCA1 degradation and consequent radioresistance.

Moreover, in the absence of both IR and RO treatment, the mice xenografted with sh*CTSS* cells displayed lower BCL2 expression than did those xenografted with shCON tumors. IR exclusively elevated CTSS expression in the tumor tissues of both shCON and sh*CTSS* xenografted mice, with a more pronounced effect in shCON tumor tissues (Fig. 5E and Supplementary Fig. S3). Moreover, the immunofluorescence (IF) data highlighted that in the irradiated shCON tumors, regions expressing elevated CTSS exhibited reduced BRCA1 expression and heightened

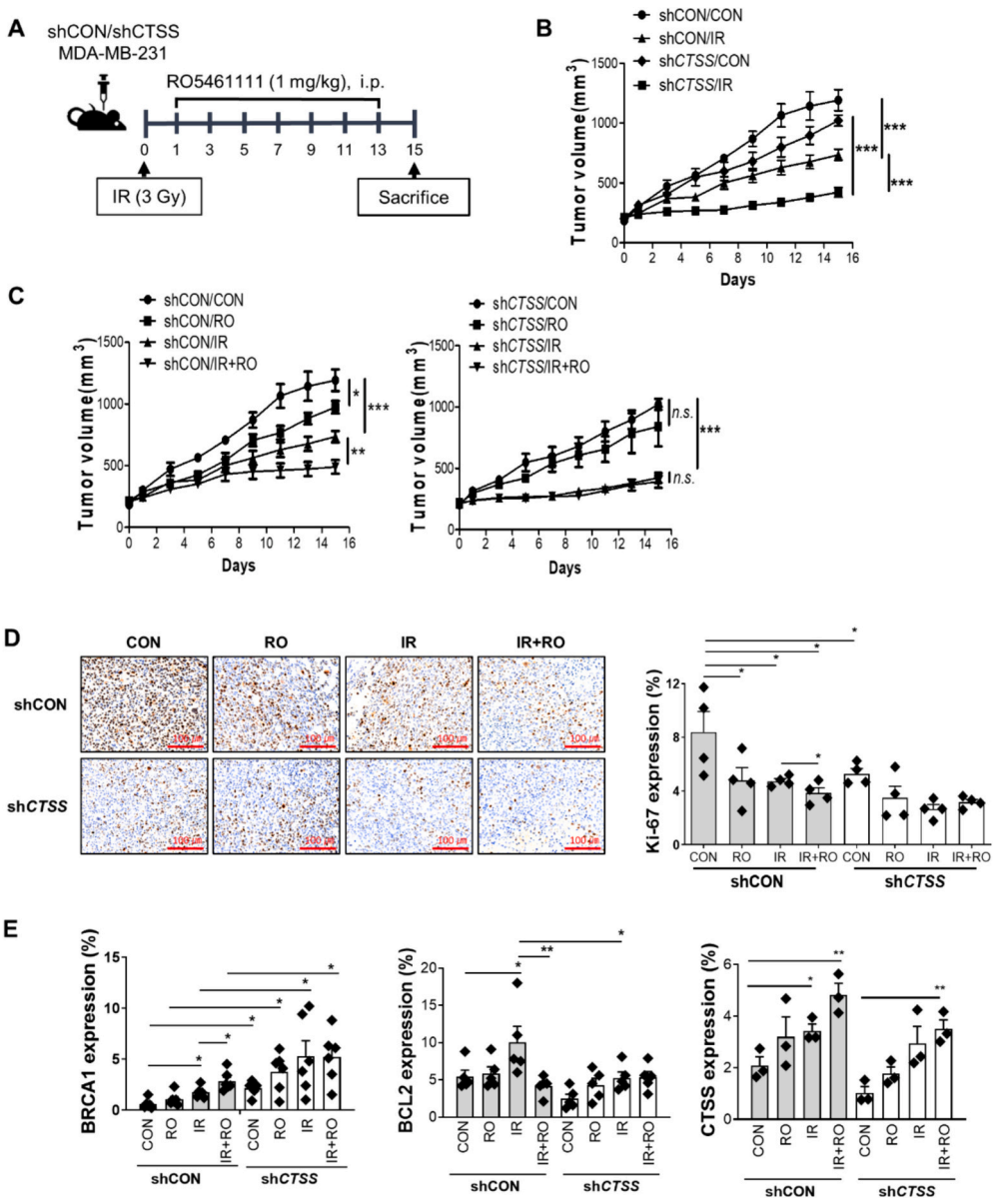


Fig. 5. Inhibiting CTSS demonstrated radiosensitization effect in a xenograft mouse model using TNBC cells harboring WT BRCA1.
(A) An experimental scheme of the tumor xenograft model; (B) Changes in the tumor volume in xenografted NOD/SCID mice ($n = 4$–7 for each group) were measured to compare the radiation effect in control and CTSS knock-down tumor model (shCON vs. shCTSS).; (C) Changes in the tumor volume in xenografted NOD/SCID mice (n = 4–7 for each group) were measured to compare the effect of CTSS inhibitor in control and CTSS knock-down tumor.; (D) Representative images of IHC analysis and quantifications of Ki67 positive areas. (E) Quantifications of BRCA1, BCL2 and CTSS positive areas by IHC analysis. Representative images are in supplementary Fig. S3.; (F) Immunofluorescence analysis of irradiated tumors of shCON and shCTSS; (G) Immunofluorescence analysis of human breast cancer patient microarray (purple; BRCA1, orange; CTSS, cyan; BCL2). Results are the means and SEM (*$p < 0.05$, ANOVA). (For interpretation of the references to colour in this figure legend, the reader is referred to the web version of this article.)

BCL2 expression. In contrast, the irradiated sh*CTSS* tumors showed relatively elevated BRCA1 expression, with areas displaying high BRCA1 expression coinciding with low BCL2 expression (Fig. 5F). To corroborate our findings, we employed antisense oligonucleotides (ASOs) tailored to target CTSS mRNA. CTSS knock-down was confirmed in 231 cells with comparison to employing si*CTSS* (Supplementary Fig. S4A and S4B). Similar to the sh*CTSS* xenograft model, the administration of a scrambled ASO (Scr-ASO) in combination with IR reduced tumor weights. However, when CTSS knockdown through the ASO approach (ASO-CTSS) was combined with IR, a notably enhanced radiosensitization effect was evident (Supplementary Fig. S4C and S4D). The breast cancer patient tissue microarray ($n = 60$) was further examined to clarify the association among the expression of CTSS, BRCA1, and BCL2 using IF. The microarray data demonstrated a down-regulation in BRCA1 expression and a significant increase in BCL2 expression in patients with high CTSS level (CTSS-H group). Moreover, TNBC patients showed higher expression of CTSS associated with a relatively lower level of BRCA1 and higher level of BCL2 compared to non-TNBC patients. Although the difference in BRCA1 level was not significant, there was a tendency for the TNBC patients to have a higher chance of radioresistance due to the overall expression pattern associated with the radioresistance mechanism of CTSS-BRCA1-BCL2 regulation (Fig. 5G).

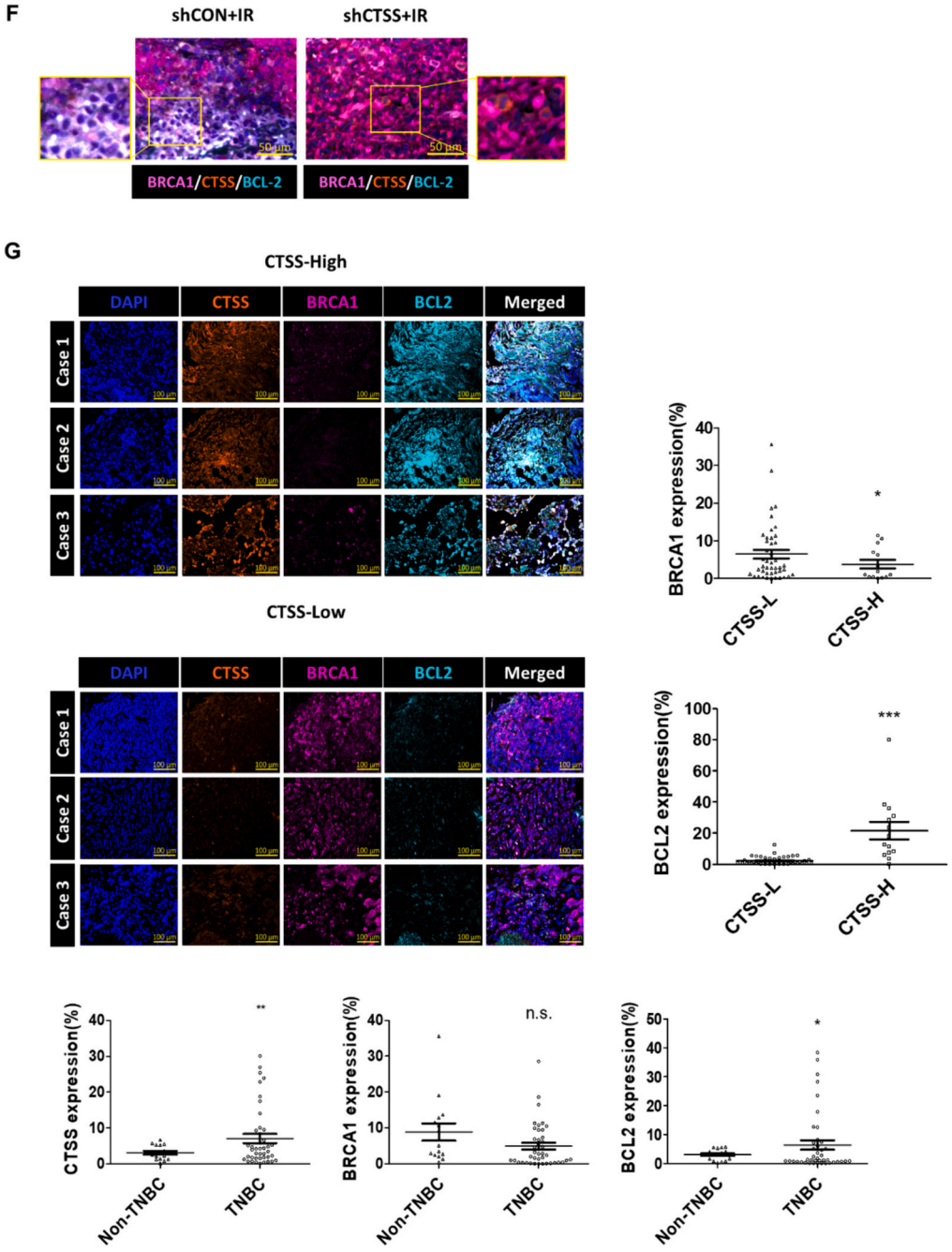


Fig. 5. (*continued*).

3. Discussion

This study introduces a novel therapeutic approach and underlying mechanisms for the treatment of TNBC, which currently lacks effective therapeutic targets. It is well-known that CTSS expression is frequently elevated in TNBC [16]. While the role of BRCA1 deficiency caused by genetic mutations and promoter hypermethylation in breast cancer is well-established, the mechanisms regulating BRCA1 protein stability in breast cancer remain poorly understood. By inhibiting CTSS, we can suppress the degradation of the BRCA1 protein, leading to enhanced ubiquitin-mediated degradation of BCL2 by BRCA1. In a previous report, we demonstrated that CTSS binds to the BRCT domain of BRCA1 and facilitates its ubiquitin-mediated degradation. This degradation process was associated with a decrease in BRCA1-mediated DNA repair activity and apoptosis [15,17]. Elevated CTSS expression is implicated in radioresistance in cancer cells., and inhibition of CTSS overcomes this radioresistance. These findings are consistent with the observed high CTSS expression in radioresistant tumors [18,19].

In this study, we examined the expression patterns of CTSS and BRCA1 in cells with WT and MT BRCT domains of BRCA1. Our findings suggest that BRCA1 expression significantly influences cell sensitivity to IR, especially in WT cells. The stability of the BRCA1 protein is controlled by phosphorylation [12]. Our results show that CTSS-mediated degradation of BRCA1 depends on its phosphorylation pattern, with phosphorylation at S1387 playing a crucial role. Moreover, inhibiting CTSS not only underscores its potential as a novel therapeutic target for TNBC patients with BRCT domain WT BRCA, but also holds significance beyond BRCA1 protein stability regulation, which makes it a promising anticancer strategy. Recent studies revealed that CTSS inhibition has shown its potential in inducing mitochondrial apoptosis of

tumor cells, inhibiting tumor invasion and metastasis and even potentiating anti-PD1 treatment [20–22].

Recent studies have suggested that BRCA1-mediated apoptosis mainly occurred in the cytoplasm [23–28]. Although the precise mechanism by which cytoplasmic BRCA1 induces cell death is not fully understood, our data indicate that CTSS-mediated degradation of BRCA1 predominantly occurs in the cytoplasm. Therefore, increased apoptosis observed with CTSS inhibitors is likely a result of stabilizing cytoplasmic BRCA1. Therefore, targeting the stabilization of cytoplasmic BRCA1 through CTSS inhibition represents a promising strategy for radiosensitization by promoting tumor apoptosis (Fig. 6).

The relationship between BRCA1 and the anti-apoptotic molecule BCL2 also explained the involvement of BRCA1 in apoptosis [14]. Our findings demonstrate that inhibiting CTSS led to suppression of BCL2 expression, along with inhibition of BRCA1 degradation, particularly at the phosphorylation site S1387. It has been reported that nuclear BRCA1 facilitated BCL2 synthesis, while cytoplasmic BRCA1 promoted the proteasomal degradation of BCL2 [14]. These findings elucidate the crucial role of cytoplasmic BRCA1 in inducing apoptosis through the degradation of BCL2 upon exposure to IR. Our investigation into the colocalization of CTSS, BRCA1, and BCL2 in the human breast cancer patient tissue microarray revealed that areas with high CTSS expression exhibited lower levels of BRCA1 and higher levels of BCL2. In contrast, areas with high BRCA1 expression showed lower levels of CTSS and BCL2. Therefore, there may be an interdependent relationship among these three molecules.

The pivotal finding from our study indicates that, in TNBC, characterized by heightened CTSS expression, the degradation of BRCA1 in the cytoplasm results in BCL2 stabilization, potentially leading to the development of radioresistance. However, restoring BRCA1 function by inhibiting CTSS in the nucleus may have adverse effects in cancer. Therefore, in cases of elevated CTSS expression, it appears crucial to selectively restore the function of BRCA1 in the cytoplasm, rather than in the nucleus, to promote apoptosis due to IR. Successful implementation of such a strategy requires further research.

In conclusion, this study presents a highly effective strategy for radiosensitization in TNBC cells, which currently lack known therapeutic targets. By inhibiting CTSS, the cytoplasmic degradation of BRCA1 was suppressed, and BCL2 degradation by BRCA1 was promoted, inducing radiosensitization. Importantly, our findings shed light on the specific phosphorylation of cytoplasmic BRCA1 by CTSS, elucidating its role in the degradation mechanism. These findings offer a new therapeutic approach for TNBC cases predominantly characterized by normal WT -BRCA1. The current drug options primarily target BRCA1 mutations, which are relatively rare (occurring in <5 % of breast cancer cases and in 10–15 % of TNBC cases).

4. Materials and methods

4.1. Cell culture and transfection

MDA-MB-231, MDA-MB-453, HCC70 (wild-type BRCA1, TNBC), HCC1937, MDA-MB-436 (BRCA1-BRCT domain mutated, low expression of BRCA1, TNBC), and MCF7 (wild-type BRCA1, non-TNBC) cells were used. Pre-designed siRNA for *CTSS* was purchased from Bioneer (Daejeon, Korea). Transient transfection was performed using Lipofectamine 3000 (Invitrogen, Carlsbad, CA, USA) according to the manufacturer's guidelines. For the generation of the *CTSS* knockdown MDA-MB-231 stable cells, cells were infected with lentiviral particles according to the manufacturer's instructions. Control shRNA lentiviral

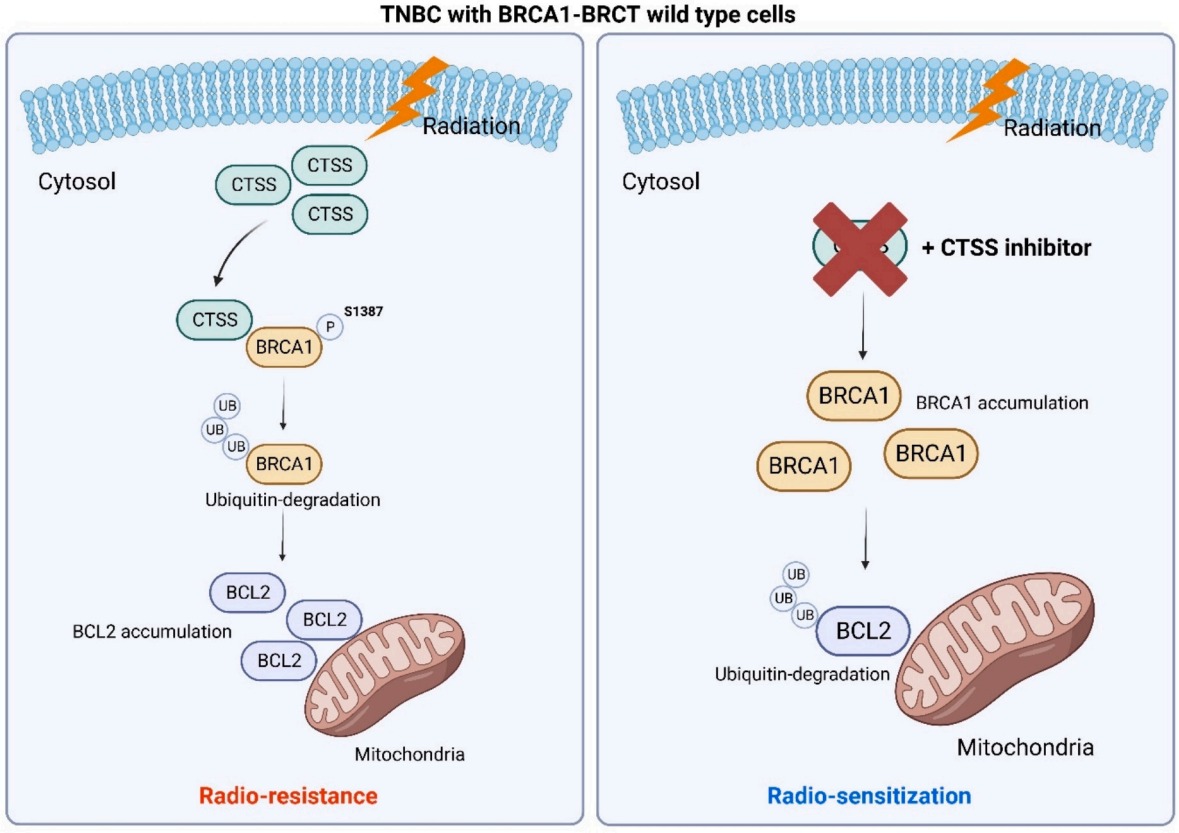


Fig. 6. Schematic illustration of molecular mechanisms of radiosensitization through CTSS inhibition in BRCA1 WT TNBC cell.
Radiation-induced CTSS recognizes phosphorylated BRCA1 at S1387 and induces it unbiquitin-mediated degradation. Increased proteolytic degradation of BRCA1 induces accumulation of anti-apoptotic BCL2 leading to radio-resistance. Inhibition of CTSS may provide a novel therapeutic strategy of radiosensitization through increased BRCA1-induced apoptosis of cancer cells harboring WT BRCA1.

particles (#sc-108,080) and *CTSS* shRNA lentiviral particles (#sc-29,940-v) were obtained from Santa Cruz Biotechnology (CA, USA). ATM-proficient GM00637 and ATM-deficient GM05849 fibroblast cells were used.

4.2. Treatment of CTSS inhibitors

Cells were treated with the CTSS-specific inhibitor *Z*-FL-COCHO (ZFL, #A13502), which was purchased from AdooQ-bioscience (CA, USA). RO5461111 was provided by Roche (Basel, Switzerland).

4.3. Cellular fractionation

Cellular fractionation was performed using a subcellular protein fractionation kit (#78841, Thermo Fisher Scientific, Waltham, MA, USA) according to the manufacturer's instructions.

4.4. Immunoblotting and immunoprecipitation

For immunoprecipitation, cells (1×10^6) were lysed in immunoprecipitation buffer (50 mM HEPES, pH 7.6, 150 mM NaCl, 5 mM EDTA, 0.1 % Nonidet P-40). After centrifugation (30 min at 15,000 g) to remove particulate material, supernatants were incubated with antibodies (1:50) against ubiquitin with constant agitation at 4 °C. Immunocomplexes were precipitated with protein A/G PLUS-agarose (#sc-2003; Santa Cruz Biotechnology) and analyzed by sodium dodecyl sulfate-polyacrylamide gel electrophoresis. The information of antibodies used for western blotting are provided in Supplementary Table S1.

4.5. Flow cytometry (FACS)

Cells were washed two times with 1× PBS, separated using trypsin-EDTA (Gibco-Invitrogen, Paisley, Scotland, UK), and centrifuged at 13000 rpm for 3 min at 4 °C. After adding 1 mL of 1× PBS and 10 μL of propidium iodide 5 mM (#P4170; Sigma-Aldrich) to polystyrene round-bottom tubes, the samples were detected by a FACs flow cytometer (BD Bioscience, San Jose, CA, USA).

4.6. CTSS protease activity

CTSS protease activity using a cell system was measured with assay kits for CTSS (#ab65307) purchased from Abcam (Cambridge, MA, USA). The enzymatic assay itself was conducted according to the manufacturer's instructions. Relative fluorescent unit (RFU) values were analyzed using the Infinite F200 PRO microplate multi-reader (Tecan, equipped at Ewha Drug Development Research Core Center).

4.7. Gadd45 promoter assay

Gadd45 WT-luc plasmid was purchased from Addgene (Cambridge, MA, USA). The Gadd45 promoter activity was measured using a luciferase assay system kit (# E4030, Promega, Madison, WI, USA) according to the manufacturer's instructions.

4.8. Irradiation

Cells were plated in 60-mm dishes in culture medium and incubated at 37 °C in a humidified 5 % CO_2 atmosphere until 70–80 % confluent. Cells were then exposed to γ-rays with a ^{137}Cs γ-ray source (Elan 3000, Atomic Energy of Canada, Ontario, Canada) at a dose rate of 3.81 Gy/min.

4.9. Tumor xenograft experiment using NOD-SCID mice

A single-cell suspension of control or CTSS knockdown stable MDA-MB-231 cells (1×10^7 cells, shCON or sh*CTSS*) was injected subcutaneously into the hind legs of 5-week-old female NOD-SCID mice (Koatech, Pyeongtaek, Korea). A single dose of 3 Gy was delivered with a local, regional application using a ^{137}Cs irradiator (Biobeam8000, Gamma Service Medical, equipped at the Korea Institute of Radiological and Medical Science). One day after irradiation, the NOD-SCID mice were treated with 1 mg/kg RO every day intraperitoneally for 2 weeks. Tumor growth was monitored 2–3 times per week to assess treatment efficacy starting 2 weeks after the MDA-MB-231 cells were injected. The long diameter [4] and short diameter (SD) were measured to calculate tumor volume as volume = $(LD \times SD^2)/2$. According to the IACUC, the tumor size must not exceed 20 mm at the largest diameter in mice, as was demonstrated in this study. The animal studies were approved by the Institutional Animal Care and Use Committee (IACUC) of Ewha Womans University [IACUC 21-027].

4.10. Tissue histology and immunohistochemical (IHC) and immunofluorescence (IF) staining

For tissue preparation, deparaffinized sections were submerged in antigen-retrieval buffer (#ab93678; Abcam) for 30 min and next incubated with 0.3 % (*v*/v) hydrogen peroxide in methanol for 10 min. The sections were blocked in normal goat serum at 37 °C incubator for 1 h and immunostained overnight at 4 °C with primary antibodies. Detailed information for each staining process is in Additional file 1.

4.11. Proximity ligation assay (PLA)

For PLA, Duolink® PLA Reagents (Sigma) were used according to the manufacturer's instructions with primary anti-BRCA1, anti-CTSS, and anti-BLC2 antibodies. For each experiment, negative controls were analyzed without primary antibodies or PLA probes. Nuclear immunofluorescence images were obtained using a Zeiss microscope Apotome (Cal Zeiss), equipped at Ewha Drug Development Research Core Center. Automated identification and quantification of the foci were analyzed using Image J software (NIH).

4.12. Human tissues analysis

Human breast cancer tissue slides were purchased from US Biomax. For antigen retrieval, the slides were placed in 10 mM citric acid buffer (pH 6.0) and heated at 100 °C for 10 min. The slides were incubated overnight at 4 °C with antibodies. Image quantification was performed using an image analyzer (Image J, NIH). All statistical analyses of the images were performed using GraphPad Prism software 5.0 (GraphPad Software, San Diego, CA, USA).

4.13. Statistical analysis

Data are expressed as mean ± standard deviation (SD) or standard error of the mean (SEM) for in-vitro experiments or in-vivo experiments, respectively. Statistical significance was determined by Student's *t*-test or one-way ANOVA (Newman-Keuls test). The differences were considered significant if the p value was <0.05. The ANOVA test was performed using GraphPad Prism software 5.0.

Funding

This work was supported by a grant from the National Research Foundation of Korea (NRF) grants (NRF-2020R1A2C3013255, 2018R1A5A2025286, and 2020M2D9A2093974), funded by the Korean government (Ministry of Science and ICT).

CRediT authorship contribution statement

Gil-Im Mun: Validation, Methodology, Investigation, Data curation.

Eun Choi: Writing – original draft, Validation, Methodology, Investigation, Formal analysis, Data curation. **Hee Jin:** Data curation, Formal analysis, Methodology, Validation. **Seul-Ki Choi:** Validation, Methodology, Investigation. **Seoyoung Kim:** Validation, Methodology, Investigation. **Junghyun Kim:** Validation, Methodology. **Chaerin Kang:** Methodology. **Hye Lim Oh:** Methodology. **Hae-June Lee:** Methodology. **Dae-Ro Ahn:** Validation, Resources, Methodology, Investigation. **Yun-Sil Lee:** Writing – review & editing, Writing – original draft, Supervision, Resources, Project administration, Funding acquisition, Conceptualization.

Declaration of competing interest

The authors declare that they have no known competing financial interests or personal relationships that could have appeared to influence the work reported in this paper.

TNBC cell lines were exposed to irradiation (10 Gy) after pre-treatment with CTSS inhibitors; RO5461111 (RO) and *Z*-FL-COCHO (Z-FL). TNBC cell lines with wild-type BRCA1 (WT); MDA-MB-231 (231) & HCC70 and mutant BRCA1 (MT); MDA-MB-436 (436) & HCC1937 (1937). (A) Western blot analysis and the quantification of cleaved-PARP1 induction; (B) Cell death was evaluated with PI staining. Results are the means and SD ($*p < 0.05$, ANOVA).

Data availability

Any further information or requests for reagents and resources should be directed to the corresponding authors.

Appendix A. Supplementary data

Supplementary data to this article can be found online at https://doi.org/10.1016/j.bbadis.2024.167523.

References

[1] W.D. Foulkes, I.E. Smith, J.S. Reis-Filho, Triple-negative breast cancer, N. Engl. J. Med. 363 (2010) 1938–1948.

[2] B.S. Yadav, P. Chanana, S. Jhamb, Biomarkers in triple negative breast cancer: a review, World Journal of Clinical Oncology 6 (2015) 252.

[3] G. Bianchini, J.M. Balko, I.A. Mayer, M.E. Sanders, L. Gianni, Triple-negative breast cancer: challenges and opportunities of a heterogeneous disease, Nature Reviews Clin. Oncol. 13 (2016) 674–690.

[4] E. Lips, L. Mulder, A. Oonk, L. Van Der Kolk, F. Hogervorst, A. Imholz, J. Wesseling, S. Rodenhuis, P. Nederlof, Triple-negative breast cancer: BRCAness and concordance of clinical features with BRCA1-mutation carriers, Br. J. Cancer 108 (2013) 2172–2177.

[5] J. Chen, Ataxia telangiectasia-related protein is involved in the phosphorylation of BRCA1 following deoxyribonucleic acid damage, Cancer Res. 60 (2000) 5037–5039.

[6] D. Cortez, Y. Wang, J. Qin, S.J. Elledge, Requirement of ATM-dependent phosphorylation of brca1 in the DNA damage response to double-strand breaks, Science 286 (1999) 1162–1166.

[7] M. Gatei, B.-B. Zhou, K. Hobson, S. Scott, D. Young, K.K. Khanna, Ataxia telangiectasia mutated (ATM) kinase and ATM and Rad3 related kinase mediate phosphorylation of Brca1 at distinct and overlapping sites: in vivo assessment using phospho-specific antibodies, J. Biol. Chem. 276 (2001) 17276–17280.

[8] J.-S. Lee, K.M. Collins, A.L. Brown, C.-H. Lee, J.H. Chung, hCds1-mediated phosphorylation of BRCA1 regulates the DNA damage response, Nature 404 (2000) 201–204.

[9] R.S. Tibbetts, D. Cortez, K.M. Brumbaugh, R. Scully, D. Livingston, S.J. Elledge, R. T. Abraham, Functional interactions between BRCA1 and the checkpoint kinase ATR during genotoxic stress, Genes Dev. 14 (2000) 2989–3002.

[10] B. Xu, A.H. O'Donnell, S.-T. Kim, M.B. Kastan, Phosphorylation of serine 1387 in Brca1 is specifically required for the Atm-mediated S-phase checkpoint after ionizing irradiation, Cancer Res. 62 (2002) 4588–4591.

[11] A.D. Choudhury, H. Xu, R. Baer, Ubiquitination and proteasomal degradation of the BRCA1 tumor suppressor is regulated during cell cycle progression, J. Biol. Chem. 279 (2004) 33909–33918.

[12] J.L. Kim, G.H. Ha, L. Campo, M.F. Denning, T.B. Patel, C. Osipo, S.Y. Lin, E. K. Breuer, The role of Rak in the regulation of stability and function of BRCA1, Oncotarget 8 (2017) 86799–86815.

[13] E. Choi, G.-I. Mun, J. Lee, H. Lee, J. Cho, Y.-S. Lee, BRCA1 deficiency in triple-negative breast cancer: protein stability as a basis for therapy, Biomed. Pharmacother. 158 (2023) 114090.

[14] M.F. Montenegro, R. González-Guerrero, L. Sánchez-del-Campo, A. Piñero-Madrona, J. Cabezas-Herrera, J.N. Rodríguez-López, PRMT1-dependent methylation of BRCA1 contributes to the epigenetic defense of breast cancer cells against ionizing radiation, Sci. Rep. 10 (2020) 13275.

[15] S. Kim, H. Jin, H.-R. Seo, H.J. Lee, Y.-S. Lee, Regulating BRCA1 protein stability by cathepsin S-mediated ubiquitin degradation, Cell Death & Differentiation 26 (2019) 812–825.

[16] J. Gautam, Y.K. Bae, J.-A. Kim, Up-regulation of cathepsin S expression by HSP90 and 5-HT 7 receptor-dependent serotonin signaling correlates with triple negativity of human breast cancer, Breast Cancer Res. Treat. 161 (2017) 29–40.

[17] K. Miyahara, N. Takano, Y. Yamada, H. Kazama, M. Tokuhisa, H. Hino, K. Fujita, E. Barroga, M. Hiramoto, H. Handa, M. Kuroda, T. Ishikawa, K. Miyazawa, BRCA1 degradation in response to mitochondrial damage in breast cancer cells, Sci. Rep. 11 (2021) 8735.

[18] H.R. Seo, S. Bae, Y.S. Lee, Radiation-induced cathepsin S is involved in radioresistance, Int. J. Cancer 124 (2009) 1794–1801.

[19] X.Y. Wang, N.M. Beeraka, N.N. Xue, H.M. Yu, Y. Yang, M.X. Liu, V.N. Nikolenko, J. Q. Liu, D. Zhao, Identification of a three-gene prognostic signature for radioresistant esophageal squamous cell carcinoma, World J. Clin. Oncol. 14 (2023) 13–26.

[20] E. Dheilly, E. Battistello, N. Katanayeva, S. Sungalee, J. Michaux, G. Duns, S. Wehrle, J. Sordet-Dessimoz, M. Mina, J. Racle, P. Farinha, G. Coukos, D. Gfeller, A. Mottok, R. Kridel, B.E. Correia, C. Steidl, M. Bassani-Sternberg, G. Ciriello, V. Zoete, E. Oricchio, Cathepsin S Regulates Antigen Processing and T Cell Activity in Non-Hodgkin Lymphoma, Cancer Cell 37 (2020) 674–689, e612.

[21] M. Fei, L. Zhang, H. Wang, Y. Zhu, W. Niu, T. Tang, Y. Han, Inhibition of Cathepsin S induces mitochondrial apoptosis in glioblastoma cell lines through mitochondrial stress and autophagosome accumulation, Front. Oncol. 10 (2020).

[22] R.D.A. Wilkinson, A. Young, R.E. Burden, R. Williams, C.J. Scott, A bioavailable cathepsin S nitrile inhibitor abrogates tumor development, Mol. Cancer 15 (2016) 29.

[23] E. Dizin, I. Irminger-Finger, Negative feedback loop of BRCA1–BARD1 ubiquitin ligase on estrogen receptor alpha stability and activity antagonized by cancer-associated isoform of BARD1, Int. J. Biochem. Cell Biol. 42 (2010) 693–700.

[24] M. Fabbro, S. Schuechner, W.W.Y. Au, B.R. Henderson, BARD1 regulates BRCA1 apoptotic function by a mechanism involving nuclear retention, Exp. Cell Res. 298 (2004) 661–673.

[25] W. Fan, S. Jin, T. Tong, H. Zhao, F. Fan, M.J. Antinore, B. Rajasekaran, M. Wu, Q. Zhan, BRCA1 regulates GADD45 through its interactions with the OCT-1 and CAAT motifs*, J. Biol. Chem. 277 (2002) 8061–8067.

[26] S.C. Hedgepeth, M.I. Garcia, L.E. Wagner, A.M. Rodriguez, S.V. Chintapalli, R. R. Snyder, G.D.V. Hankins, B.R. Henderson, K.M. Brodie, D.I. Yule, D.B. van Rossum, D. Boehning, The BRCA1 tumor suppressor binds to inositol 1,4,5-trisphosphate receptors to stimulate apoptotic calcium release*, J. Biol. Chem. 290 (2015) 7304–7313.

[27] M. Thangaraju, S.H. Kaufmann, F.J. Couch, BRCA1 facilitates stress-induced apoptosis in breast and ovarian Cancer cell lines*, J. Biol. Chem. 275 (2000) 33487–33496.

[28] W. Zhang, J. Luo, F. Chen, F. Yang, W. Song, A. Zhu, X. Guan, BRCA1 regulates PIG3-mediated apoptosis in a p53-dependent manner, Oncotarget 6 (2015) 7608.